ISSN 1070-3284, Russian Journal of Coordination Chemistry, 2013, Vol. 39, No. 11, pp. 764–770. © Pleiades Publishing, Ltd., 2013.
Original Russian Text © M.A. Ivanov, A.S. Zaeva, A.V. Gerasimenko, A.V. Ivanov, 2013, published in Koordinatsionnaya Khimiya, 2013, Vol. 39, No. 11, pp. 656–662.

Platinum(II) *cyclo*-Hexamethylenedithiocarbamate Complex, $[Pt\{S_2CN(CH_2)_6\}_2]$ and Its Solvated Form, $[Pt\{S_2CN(CH_2)_6\}_2] \cdot CHCl_3$: Crystal and Molecular Structures, ^{13}C CP/MAS NMR Data, and Thermal Behavior

M. A. Ivanov[a], A. S. Zaeva[a], A. V. Gerasimenko[b], and A. V. Ivanov[a], *

[a] *Institute of Geology and Nature Management, Far East Branch, Russian Academy of Sciences, Blagoveshchensk, 675000 Russia*

[b] *Institute of Chemistry, Far East Branch, Russian Academy of Sciences, Vladivostok, 690022 Russia*

**e-mail: alexander.v.ivanov@chemist.com*

Received March 13, 2013

Abstract—Platinum(II) *cyclo*-hexamethylenedithiocarbamate (HmDtc) complex, $[Pt\{S_2CN(CH_2)_6\}_2]$ (**I**), and its solvated form, $Pt\{S_2CN(CH_2)_6\}_2] \cdot CHCl_3$ (**II**), are synthesized and characterized by the ^{13}C MAS NMR data. The HmDtc ligands in structure **I** are not equivalent, whereas the solvation of the complex is accompanied by the structural unification of the initially nonequivalent HmDtc ligands. In addition, the spectra are characterized by the ^{13}C–^{195}Pt spin-spin coupling. The noncentrosymmetric molecular structure of compound **I** determined by X-ray diffraction analysis includes two nonequivalent dithiocarbamate ligands coordinated by the metal in the S,S'-bidentate mode. The central atom forming the $[PtS_4]$ chromophore (intraorbital *dsp*^{2}-hybrid state of platinum) shifts from the plane of four sulfur atoms by 0.07 Å and finds itself in the vertex of the flattened tetragonal pyramid. The seven-membered heterocycles $–N(CH_2)_6$ of the HmDtc ligands are oppositely directed in space relative to the $[S_4]$ plane (*trans* orientation). The thermal behavior of compounds **I** and **II** are studied by simultaneous thermal analysis. In both cases, the final product of the multistage thermal destruction of the complexes is reduced metallic platinum.

DOI: 10.1134/S1070328413110031

INTRODUCTION

Areas of the practical application of dithiocarbamates are fairly diverse [1–7]. Interest in the platinum(II) complexes containing dithiocarbamate ligands is due, to a great extent, to the medical aspect of their use [8–12] and associated with the search for compounds characterized by a high antitumor activity and a lowered toxicity compared to cisplatin. Therefore, the synthesis of new platinum(II) complexes and the study of their structures and properties are of significant interest [13–18]. Although many heteroligand platinum(II) complexes including dithiocarbamate groups have been described, the structural data on the platinum dithiocarbamates themselves are scarce [16–18].

We have earlier characterized single-crystal cooperite (natural mineral of platinum, PtS [19] in which platinum forms the $[PtS_4]$ chromophore) by the EPR and ^{195}Pt NMR spectroscopy (both static and MAS). A structurally similar situation was observed for the platinum dialkyldithiophosphate complexes [20–23].

In continuation of our studies of the platinum(II) complexes with dithio reagents, we synthesized crystalline platinum(II) *cyclo*-hexamethylenedithiocarbamate, $[Pt\{S_2CN(CH_2)_6\}_2]$ (**I**), and its chloroform-solvated form, $[Pt\{S_2CN(CH_2)_6\}_2] \cdot CHCl_3$ (**II**). The preparatively isolated compounds were characterized by the ^{13}C MAS NMR and X-ray diffraction analysis data. The thermal behavior of compounds **I** and **II** was studied by simultaneous thermal analysis (STA).

EXPERIMENTAL

Synthesis of I was carried out by the interaction of aqueous solutions of $K_2[PtCl_6]$ (Merck) and $Na\{S_2CN(CH_2)_6\} \cdot 2H_2O$.[1] The reaction mixture was heated to 60°C and left to stay overnight. The obtained light green precipitate was filtered off, washed with water, and dried on the filter. Yellow crystals of compounds **I** and **II** were obtained from chloroform by the slow and fast evaporation of the solvent, respectively.

^{13}C MAS NMR (δ, ppm): $[Pt\{S_2CN(CH_2)_6\}_2]$ (**I**): 209.8 (127)*, 209.4 (132)* (1 : 1, $–S_2CN=$); 51.4, 50.3, 49.7, 48.2 (1 : 1 : 1 : 1, $=NCH_2–$); 30.5, 30.0, 28.5, 27.4,

---

[1] The original sodium N,N-*cyclo*-hexamethylenedithiocarbamate was synthesized by the reaction of carbon disulfide (Merck) and hexamethyleneimine (Aldrich) in an alkaline medium [24].

27.0 (1 : 2 : 2 : 2 : 1, $-CH_2-$); $[Pt\{S_2CN(CH_2)_6\}_2] \cdot CHCl_3$ (**II**): 209.9 (101)*, (42)** ($-S_2CN=$); 50.6 (33)**, 48.2 (31)** (1 : 1, $=NCH_2-$); 31.0, 29.7, 27.4, 26.9 (1 : 1 : 1 : 1, $-CH_2-$); 77.6 ($CHCl_3$); $Na\{S_2CN(CH_2)_6\} \cdot 2H_2O$ (1 : 2 : 2 : 2): 206.3 ($-S_2CN=$); 60.3, 55.5 (1 : 1, $=NCH_2-$); 29.8, 27.0, 26.2, 24.9 (1 : 1 : 1 : 1, $-CH_2-$). (* Spin-spin coupling (SSC) constants ^2J ($^{13}C-^{195}Pt$), in Hz; ** asymmetric $^{13}C-^{14}N$ doublets [25, 26], in Hz.)

^{13}C MAS NMR spectra were recorded on a CMX-360 (Agilent/Varian/Chemagnetics Infinity-Plus) spectrometer with a working frequency of 90.52 MHz, a superconducting magnet ($B_0 = 8.46$ T), and Fourier transform. The proton cross-polarization, the $^{13}C-^1H$ decoupling effect, and a radiofrequency field at the resonance frequency of protons were used [27]. Samples (~100 mg) were placed in a 4.0-mm ceramic rotor of ZrO_2. Rotation at a magic angle at a frequency of 5700–6700(1) Hz was used in ^{13}C MAS NMR measurements (scan number 5800–12900; duration of proton $\pi/2$ pulses 3.3–4.9 μs, $^1H-^{13}C$ contact time 2.5 ms, interval between pulses 3.0–5.0 s). The ^{13}C isotropic chemical shifts (δ) are given relative to one of the components of crystalline adamantane used as an external standard [28] (δ = 38.48 ppm relative to tetramethylsilane [29]). To refine the chemical shifts and intensities of the overlapped ^{13}C resonance signals, the fragment-to-fragment spectra simulation was used (Spinsight program), taking into account the positions and widths of the lines and the Lorentzian and Gaussian contributions to the line shapes.

X-ray diffraction analysis of I was performed on a BRUKER Kappa APEX II CCD diffractometer (MoK_α radiation, $\lambda = 0.71073$ Å, graphite monochromator, crystal–detector distance 45 mm) from a prismatic single crystal at 170(2) K. Intensity data were corrected for absorption using the indices of equivalent reflections. The structure was solved by a direct method and refined by least squares (for F^2) in the anisotropic approximation for non-hydrogen atoms. The positions of hydrogen atoms were calculated geometrically and included into the refinement in the riding model.

The data were collected and edited and the unit cell parameters were refined using the APEX2 [30] and SAINT programs [31]. The calculations on structure determination and refinement were performed using the SHELXTL/PC programs [32]. The main crystallographic data and the results of refinement of structure **I** are given in Table 1. Selected bond lengths and angles are given in Table 2. The coordinates of atoms, bond lengths, and angles were deposited with the Cambridge Crystallographic Data Centre (no. 913330; deposit@ccdc.cam.ac.uk or http://www.ccdc.cam.ac.uk).

Table 1. Crystallographic data and the experimental and refinement parameters for structure **I**

Parameter	Value
Empirical formula	$C_{14}H_{24}N_2S_4Pt$
FW	543.68
Crystal system	Monoclinic
Space group	$P2_1/c$
a, Å	8.3682(2)
b, Å	16.5979(3)
c, Å	13.0753(3)
β, deg	102.665(1)
V, Å^3	1771.90(7)
Z	4
ρ_{calcd}, g/cm^3	2.038
μ, mm^{-1}	8.385
F(000)	1056
Crystal shape (size, mm)	Prism (0.50 × 0.38 × 0.25)
Data collection over θ range, deg	2.01–31.09
Ranges of reflection indices	$-12 \le h \le 12, -24 \le k \le 23, -18 \le l \le 18$
Number of measured reflections	72784
Number of independent reflections (R_{int})	5547 (0.0348)
Reflections with $I > 2\sigma(I)$	5133
Refinement variables	190
Goodness-of-fit	1.068
R factors for $F^2 > 2\sigma(F^2)$	$R_1 = 0.0148, wR_2 = 0.0366$
R factors for all reflections	$R_1 = 0.0174, wR_2 = 0.0353$
Residual electron density (min/max), e Å^{-3}	−0.975/0.839

Thermal behavior of compounds **I** and **II** was studied by the STA method with simultaneous recording of thermogravimetry (TG) and differential scanning calorimetry (DSC) curves. The study was carried out on an STA 449C Jupiter instrument (NETZSCH) in corundum crucibles with caps with a hole providing a vapor pressure of 1 atm during the thermal decomposition of the sample. The heating rate was 5°C/min upto 1100°C under argon. The weight of the samples was 2.465–9.165 mg. For the more distinct elucidation of thermal effects, an additional detection at the initial stage was carried out in aluminum crucibles (heating rate 10°C/min to 600°C, sample weight ~9 mg). The accuracy of temperature measurements was ±0.7°C, and that of the weight changes was $\pm 1 \times 10^{-4}$ mg. When recording the TG and DSC curves, the correction file and temperature and sensitivity calibrations for the specified temperature program and heating rate were used. The melting points of compounds **I** and **II** were independently measured in glass capillaries on a PTP(M) instrument (Khimlaborpribor, Russia).

Table 2. Selected bond lengths (d) and the bond (ω) and torsion (φ) angles in structure **I**

Bond	d, Å	Bond	d, Å
Pt(1)–S(1)	2.3177(5)	Pt(1)–S(3)	2.3187(4)
Pt(1)–S(2)	2.3131(4)	Pt(1)–S(4)	2.3147(5)
S(1)–C(1)	1.725(2)	S(3)–C(8)	1.728(2)
S(2)–C(1)	1.730(2)	S(4)–C(8)	1.723(2)
N(1)–C(1)	1.312(2)	N(2)–C(8)	1.318(2)
N(1)–C(2)	1.472(2)	N(2)–C(9)	1.471(2)
N(1)–C(7)	1.471(2)	N(2)–C(14)	1.471(2)
Angle	ω, deg	Angle	ω, deg
S(1)Pt(1)S(2)	75.37(2)	S(3)Pt(1)S(4)	75.27(2)
S(1)Pt(1)S(3)	104.87(2)	S(2)Pt(1)S(4)	104.33(2)
S(1)Pt(1)S(4)	178.22(2)	S(2)Pt(1)S(3)	174.84(2)
S(1)C(1)S(2)	110.04(10)	S(4)C(8)S(3)	110.13(10)
Pt(1)S(1)C(1)	87.17(6)	Pt(1)S(3)C(8)	86.95(6)
Pt(1)S(2)C(1)	87.20(6)	Pt(1)S(4)C(8)	87.19(6)
N(1)C(1)S(1)	125.37(13)	N(2)C(8)S(3)	124.79(13)
N(1)C(1)S(2)	124.58(13)	N(2)C(8)S(4)	125.07(14)
C(1)N(1)C(2)	121.1(2)	C(8)N(2)C(9)	119.9(2)
C(1)N(1)C(7)	120.0(2)	C(8)N(2)C(14)	121.3(2)
C(2)N(1)C(7)	118.9(2)	C(9)N(2)C(14)	118.8(2)
Angle	φ, deg	Angle	φ, deg
Pt(1)S(1)S(2)C(1)	174.65(10)	Pt(1)S(3)S(4)C(8)	–172.42(10)
S(1)Pt(1)C(1)S(2)	175.14(9)	S(3)Pt(1)C(8)S(4)	–173.13(9)
S(1)C(1)N(1)C(2)	3.2(2)	S(3)C(8)N(2)C(9)	5.0(2)
S(1)C(1)N(1)C(7)	–176.54(13)	S(3)C(8)N(2)C(14)	–178.15(14)
S(2)C(1)N(1)C(2)	–175.43(13)	S(4)C(8)N(2)C(9)	–174.24(13)
S(2)C(1)N(1)C(7)	4.9(2)	S(4)C(8)N(2)C(14)	2.6(3)

RESULTS AND DISCUSSION

The ^{13}C MAS NMR spectra of compounds **I** and **II** (Fig. 1) include the resonance signals from the dithiocarbamate groups and carbon atoms in the seven-membered hexamethyleneimine heterocycles $-N(CH_2)_6$. In addition, the spectrum of compound **II** (Fig. 1b) contains the signal assigned to the chloroform molecule: it follows from an analysis of the ratio of integral intensities that one solvate $CHCl_3$ molecule falls onto one molecule of the complex. Each of the seven structural positions of ^{13}C in the $=NC(S)S-$, $=NCH_2-$, and $-CH_2-$ groups is presented in the NMR spectrum of compound **II** (Fig. 1b) by the single resonance signal, which indirectly indicates that the HmDtc ligands in the solvated form of the complex are structurally equivalent. On the contrary, the corresponding groups of the ^{13}C resonance signals in the spectrum of complex **I** (Fig. 1a) show the structural nonequivalence of the dithiocarbamate ligands. (Thus, the solvation of complex **I** is accompanied by its structural reorganization, which appears as a drastic simplification of the ^{13}C NMR spectrum.) A specific feature of the doublet (1 : 1) of the $=NC(S)S-$ groups is the presence of side unresolved satellite signals. The mathematical simulation established the ratio of integral intensities in this group of overlapped signals to be

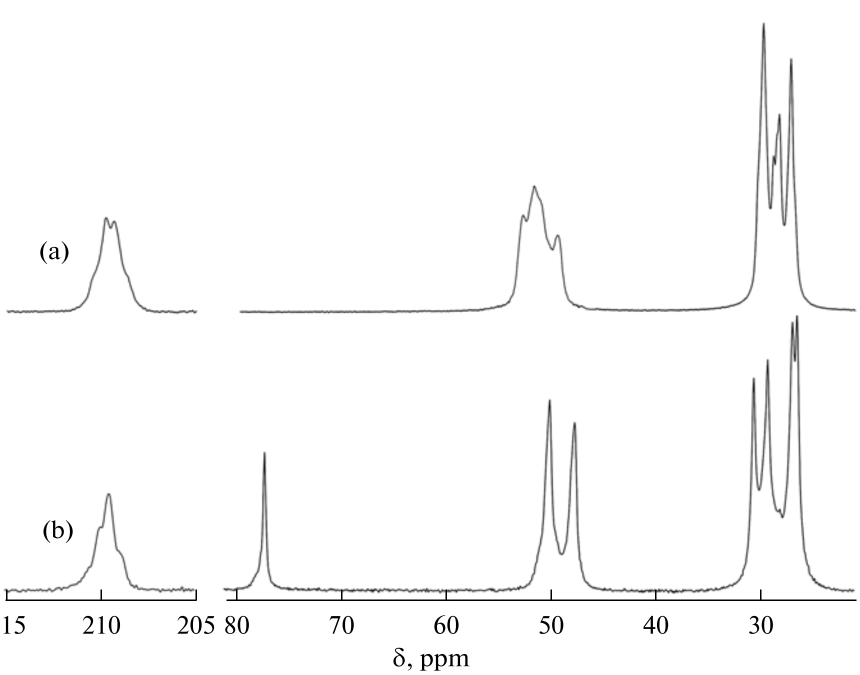

Fig. 1. MAS ^{13}C NMR spectra of polycrystalline complexes (a) **I** and (b) **II**; the scan number and the rotation frequency of the samples are 12900 and 6000 Hz for **I** and 5800 and 5700 Hz for **II**, respectively.

1 : 5 : 5 : 1. Since, natural platinum includes the ^{195}Pt nuclide (33.83 at %, $\mu = 0.60950\ \mu_N$) with the nuclear spin $I = 1/2$, each component of the doublet has two symmetrically arranged satellites (1 : 4 : 1), which is the result of the isotropic spin-spin coupling of ^{13}C nucleus with ^{195}Pt characterized by the SSC constant $^2J(^{13}\text{C}-^{195}\text{Pt})$[2]. Thus, the superposition of two triplets (1 : 4 : 1) from the nonequivalent =NC(S)S– groups results in the observed multiplet structure (1 : 5 : 5 : 1) of the discussed ^{13}C resonance signals. The unusual shape of the ^{13}C signal of the dithiocarbamate group in the solvated form of complex **II** (Fig. 1b) needs special consideration. The specifics of the discussed resonance signal is explained by the combined manifestation of two effects: (a) splitting of the ^{13}C signal into the asymmetric (1 : 2) ^{13}C–^{14}N doublet (with a constant of 42 Hz) due to the dipole-dipole interactions of the ^{13}C nucleus ($I = 1/2$) with the quadrupole ^{14}N nucleus ($I = 1$) [25, 26] and (b) SSC ^{13}C–^{195}Pt. The crystal and molecular structures of complex **I** were solved by X-ray diffraction analysis to check the conclusions about the structure of complex **I** made on the basis of the ^{13}C MAS NMR data.

The unit cell of complex **I** includes four noncentrosymmetric $[\text{Pt}\{\text{S}_2\text{CN(CH}_2)_6\}_2]$ molecules (Fig. 2). The coordination of the dithiocarbamate ligands by the central platinum atom is close to the S,S'-isobidentate mode, because the difference in the Pt–S bond lengths for each ligand is relatively small (2.3131, 2.3177 Å and 2.3147, 2.3187 Å). As expected from the ^{13}C MAS NMR data, the HmDtc ligands are structurally nonequivalent. Their bidentate coordination mode results in the formation of two four-membered metallocycles $[\text{PtS}_2\text{C}]$ joined into the bicyclic $[\text{PtS}_4\text{C}_2]$ groups by the platinum atom. The values of the PtSSC and SPtCS torsion angles (Table 2) indicate that the atoms in both cyclic groups deviate from the plane (tetrahedral distortion). The central platinum atom coordinates four sulfur atoms to form the $[\text{PtS}_4]$ chromophore (intraorbital *dsp*^{2}-hybrid state of platinum). The dihedral angle between the planes of two [PtSS] hemicycles is 5.17(3)°. Therefore, the platinum atom shifts from the plane of the $[\text{PtS}_4]$ chromophore by 0.07 Å and finds itself in the vertex of the pyramid, whose base is formed by four sulfur atoms. A similar structural effect has previously been found for the nickel(II) HmDtc complex [33]. Thus, the polyhedron of platinum is a flattened tetragonal pyramid with a rectangle in the base. The lengths of the short sides of the rectangle are determined by the intraligand distances S(1)···S(2) 2.831 and S(3)···S(4) 2.829 Å, and the lengths of the long sides are determined by the interligand distances S(1)···S(3) 3.675 and S(2)···S(4) 3.655 Å.

The small sizes of the $[\text{PtS}_2\text{C}]$ metallocycles are illustrated by the distances between the *trans*-arranged platinum and carbon atoms equal to 2.820 Å [Pt···C(1)] and 2.817 Å [Pt···C(8)], which are by

---

[2] The early appearance of the SSC (^{31}P–^{195}Pt) for similar four-membered metallocycles $[\text{PtS}_2\text{P}]$ was observed in the ^{31}P MAS NMR spectra of a series of the crystalline platinum(II) dialkyldithiophosphate complexes [20–23].

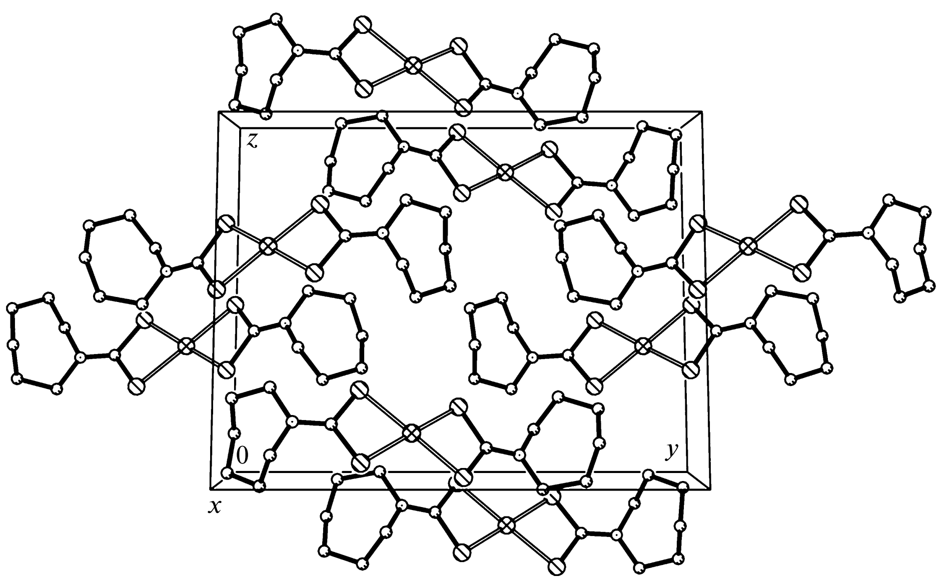

Fig. 2. Unit cell of structure **I** (projection onto the *yz* plane).

1.63 Å less than the sum of the van der Waals radii of Pt and C atoms (3.45 Å) [34, 35]. This fact indicates the high concentration of the π-electron density delocalized inside the cycles and the *trans*-annular interaction between the discussed atoms (i.e., directly through the space of the metallocycles).

The arrangement of atoms in the C_2NCS_2 groups of the HmDtc ligands is close to planar: the SCNC torsion angles do not strongly deviate from 180° or 0°. The both N–C(S)S bonds (1.312 and 1.318 Å) are noticeably stronger than $N–CH_2$ (1.471 and 1.472 Å) (Table 2). These structural regularities appear due to the mesomeric effect of the dithiocarbamate groups. In the hexamethyleneimine heterocycles $–N(CH_2)_6$, the NCC and CCC angles range from 111.0° to 115.6°; the admixing of the sp^2-hybrid state in the nitrogen atoms increases the CNC angles to 118.8°–118.9°. The heterocycles are oriented in opposite directions (*trans* orientation) relative to the $[PtS_4]$ chelate node (Fig. 3b).

In spite of the similarity of the $[PtS_4]$ chromophores in complex **I** and cooperite, the latter is characterized by the stronger Pt–S bonds (2.3108 and 2.3109 Å). In addition, all SPtS angles in cooperite are 90°, whereas in complex **I** the SPtS intraligand angles decrease to 75.37° and 75.27° and the interligand angles increase to 104.33° and 104.87°, respectively, due to the formation of the sterically strained metallocycles $[PtS_2C]$.

The TG curves of compounds **I** and **II** (Figs. 4*a* and 4*c*) show the two- and three-stage processes, respectively, of thermal destruction. The first stage of the thermolysis of compound **II** (25–100°C) is due to the desolvation of the complex with the loss of a chloroform molecule: 17.44% of the mass (calculated 18.00%). The corresponding region of the DSC curve contains the broadened endotherm with an extreme at 64°C (Fig. 4*d*). In both cases, the main mass loss (46.49 and 36.08%) is related to the active thermolysis of the dithiocarbamate moiety of the complexes in the temperature ranges 280–410°C and 295–405°C, respectively. After passing the discussed step in the TG curves, the residual mass of the samples is 53.51 and 46.48%, respectively, which substantially exceeds the expected (according to published data [21–23]) mass of PtS (calculated 41.78 and 34.26%, respectively). The results of studying the thermal behavior of platinum metal methyl-*cyclo*-hexyldithiocarbamates [36] seem to be important for the solution of the problem about the nature of the intermediate products of the thermolysis of compounds **I** and **II**. The thermolysis of the palladium(II) and platinum(II) complexes proceeds specifically: through the stage of formation of thiocyanates of these metals. In this variant, the expected mass of intermediate $Pt(SCN)_2$ should be 57.25 and 46.94%, respectively. The underestimation of the experimentally observed masses at this stage of thermolysis (53.51 and 46.48%) can be explained by the presence of some amount of PtS together with platinum(II) thiocyanate.[3] The corresponding regions of the DSC curves (Figs. 4*b* and 4*d*) show the melting endotherms for compounds **I** and **II** (after desolvation): the extrapolated melting points are equal to 299.8 and 297.1°C, respectively. For thermal destruction, these are the endotherms with extremes at 334.5, 338.1°C (**I**) and 323.0°C (**II**).

---

[3] The formation of metal sulfides in the thermolysis of the metal complexes with sulfur-containing ligands was substantiated from the thermodynamic point of view [37].

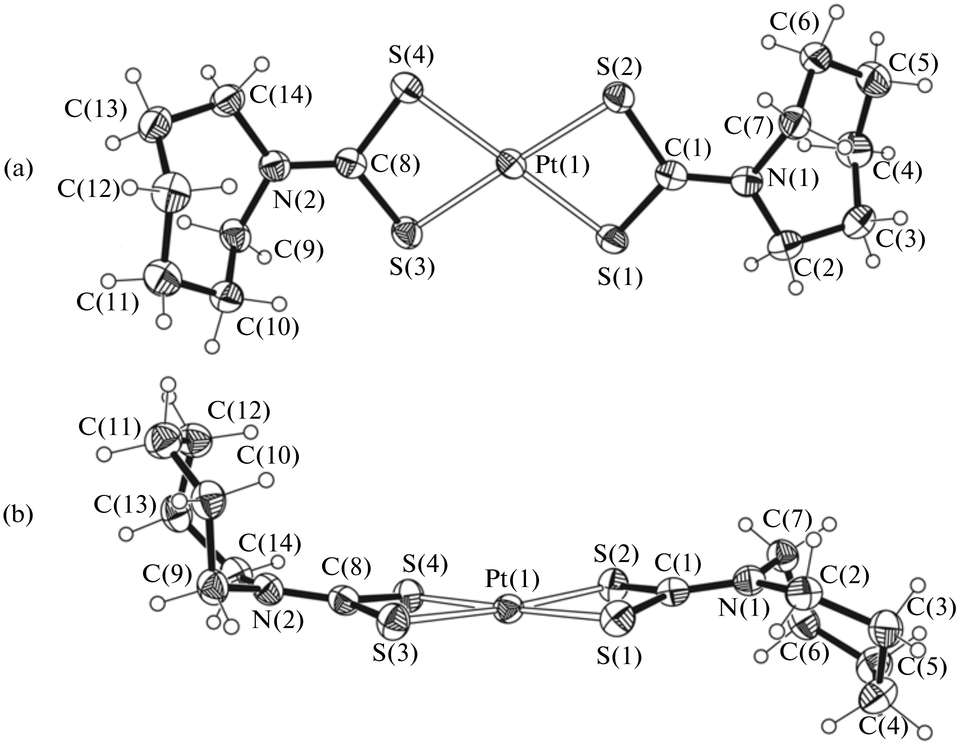

Fig. 3. (a), (b) Two projections of molecular structure **I** (displacement ellipsoids are shown at the 50% probability level).

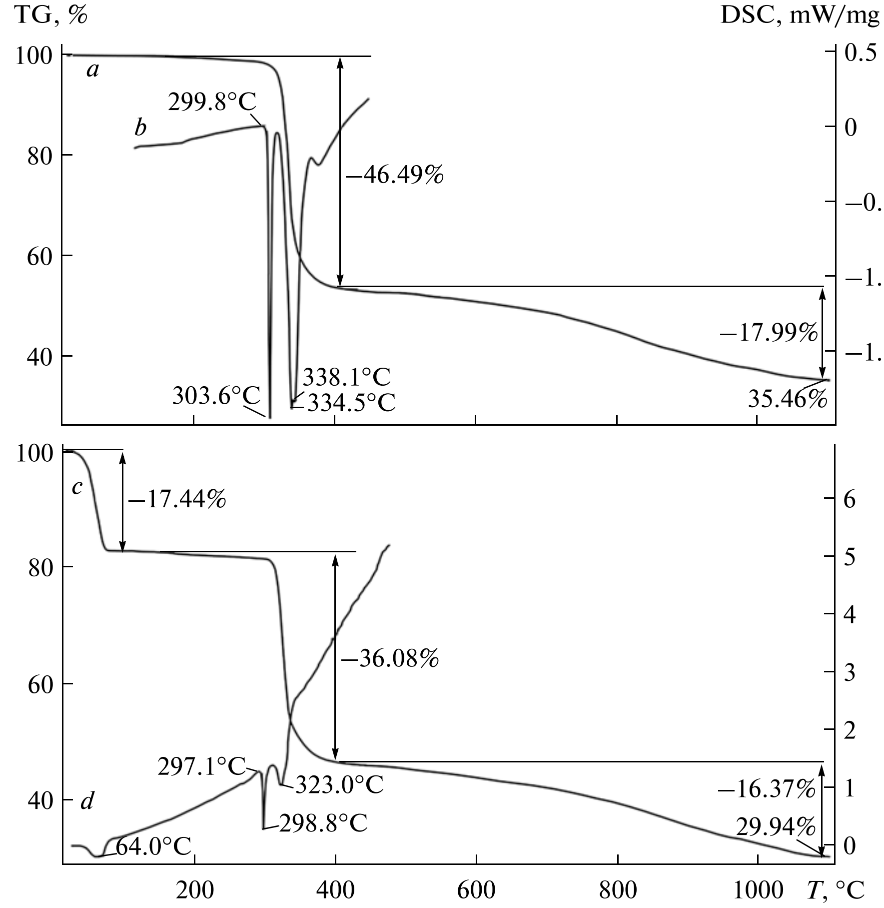

Fig. 4. (*a*), (*c*) TG and (*b*), (*d*) DSC curves for complexes **I** and **II**.

The high-temperature part of the TG curves (405–1100°C) is due to the smooth thermolysis of $Pt(SCN)_2$. The masses of the residues equal to 35.46 and 29.94%, respectively, indicate that the single final product of the thermolysis of complexes **I** and **II** is reduced metallic platinum (calculated 35.88 and 29.42%). After the end of the process, the crucibles contained fragments of the light gray dull metal foil and irregular particles with a metallic luster.

ACKNOWLEDGMENTS

The authors are grateful to Prof. O.N. Antzutkin (Luleå University of Technology, Luleå , Sweden) for the kindly presented opportunity of ^{13}C MAS NMR spectra recording.

This work was supported by the Russian Foundation for Basic Research (program "Development of Methods for Preparation of Chemical Substances and Production of New Materials," project no. 12-I-P8-01) and the Presidium of the Far East Branch of the Russian Academy of Sciences (grants nos. 12-III-A-04-040 and 13-III-V-04-045 on fundamental and applied investigations of young scientists).

REFERENCES

1. Hogarth, G., *Prog. Inorg. Chem.*, 2005, vol. 53, p. 71.
2. Srinivasan, N. and Thirumaran, S., *Superlatt. Microstruct.,* 2012, vol. 51, no. 6, p. 912.
3. Onwudiwe, D.C. and Ajibade, P.A., *Mater. Lett.,* 2011, vol. 65, nos. 21–22, p. 3258.
4. Winkelmann, K., Noviello, T., and Brooks, S., *J. Chem. Educ.*, 2007, vol. 84, no. 4, p. 709.
5. Okubo, T., Tanaka, N., Kim, K.H., et al., *Dalton Trans.,* 2011, vol. 40, no. 10, p. 2218.
6. Monti, S.M., Maresca, A., Viparelli, F., et al., *Bioorg. Med. Chem. Lett.*, 2012, vol. 22, no. 2, p. 859.
7. Carta, F., Aggarwal, M., Maresca, A., et al., *J. Med. Chem.*, 2012, vol. 55, no. 4, p. 1721.
8. Hogarth, G., *Mini-Rev. Med. Chem.*, 2012, vol. 12, no. 12, p. 1202.
9. Faraglia, G., Sindellari, L., Cerchi, V., et al., *Trans. Met. Chem.*, 1993, vol. 18, no. 1, p. 45.
10. Faraglia, G., Fregona, D., Sitran, S., et al., *J. Inorg. Biochem.*, 2001, vol. 83, no. 1, p. 31.
11. Mansouri-Torshizi, H., Eslami-Moghadam, M., Divsalar, A., et al., *Acta Chim. Sloven.*, 2011, vol. 58, no. 4, p. 811.
12. Mansouri-Torshizi, H., Saeidifar, M., Khosravi, F., et al., *Bull. Korean Chem. Soc.*, 2011, vol. 32, no. 3, p. 947.
13. Marcheselli, L., Preti, C., Tagliazucchi, M., et al., *Eur. J. Med. Chem.*, 1993, vol. 28, no. 4, p. 347.
14. Lucier, B.E.G., Reidel, A.R., and Schurko, R.W., *Can. J. Chem.*, 2011, vol. 89, no. 7, p. 919.
15. Christidis, P.C. and Rentzeperis, P.J., *Acta Crystallogr., Sect. B: Struct. Crystallogr. Cryst. Chem.*, 1979, vol. 35, no. 11, p. 2543.
16. Heath, G.A., Hockless, D.C.R., and Prenzler, P.D., *Acta Crystallogr., Sect. C: Cryst. Struct. Commun.*, 1996, vol. 52, no. 3, p. 537.
17. Oliveira, M.R.L., Rubinger, M.M.M., Guilardi, S., et al., *Polyhedron,* 2004, vol. 23, no. 7, p. 1153.
18. Amim, R.S., Oliveira, M.R.L., Perpétuo, G.J., et al., *Polyhedron,* 2008, vol. 27, no. 7, p. 1891.
19. Ivanov, A.V., Palazhchenko, V.I., Strikha, V.E., et al., *Dokl. Earth Sci.*, 2006, vol. 410, no. 7, p. 1141.
20. Rodina, T.A., Ivanov, A.V., Gerasimenko, A.V., et al., *Polyhedron,* 2011, vol. 30, no. 13, p. 2210.
21. Rodina, T.A., Lutsenko, I.A., Gerasimenko, A.V., and Ivanov, A.V., *Russ. J. Coord. Chem.*, 2009, vol. 35, no. 7, p. 534.
22. Ivanov, A.V., Rodina, T.A., Ivanov, M.A., et al., *Dokl. Phys. Chem.*, 2008, vol. 423, no. 1, p. 311.
23. Ivanov, A.V., Lutsenko, I.A., Ivanov, M.A., et al., *Russ. J. Coord. Chem.*, 2008, vol. 34, no. 8, p. 584.
24. Byr'ko, V.M., *Ditiokarbamaty* (Dithiocarbamates), Moscow: Nauka, 1984.
25. Hexem, J.G., Frey, M.H., and Opella, S.J., *J. Chem. Phys.*, 1982, vol. 77, no. 7, p. 3847.
26. Harris, R.K., Jonsen, P., and Packer, K.J., *Magn. Reson. Chem.*, 1985, vol. 23, no. 7, p. 565.
27. Pines, A., Gibby, M.G., and Waugh, J.S., *J. Chem. Phys.*, 1972, vol. 56, no. 4, p. 1776.
28. Earl, W.L. and VanderHart, D.L., *J. Magn. Reson.,* 1982, vol. 48, no. 1, p. 35.
29. Morcombe, C.R. and Zilm, K.W., *J. Magn. Reson.*, 2003, vol. 162, no. 2, p. 479.
30. *APEX2,* Madison (WI, USA): Bruker AXS, 2010.
31. *SAINT*, Madison (WI, USA): Bruker AXS, 2010.
32. Sheldrick, G.M., *Acta Crystallogr., Sect. A: Found. Crystallogr.*, 2008, vol. 64, no. 1, p. 112.
33. Starikova, Z.A., Shugam, E.A., Agre, V.M., and Oboznenko, Yu.V., *Kristallografiya,* 1972, vol. 17, no. 1, p. 111.
34. Bondi, A., *J. Phys. Chem.*, 1964, vol. 68, no. 3, p. 441.
35. Bondi, A., *J. Phys. Chem.*, 1966, vol. 70, no. 9, p. 3006.
36. Sangari, H.S., Sodhi, G.S., and Kaur, J., *Thermochim. Acta,* 1990, vol. 171, p. 49.
37. Razuvaev, G.A., Almazov, G.V., Domrachev, G.A., et al., *Dokl. Akad. Nauk SSSR*, 1987, vol. 294, no. 1, p. 141.

Translated by E. Yablonskaya